

PAPER • OPEN ACCESS

## Temperature activation of indirect exciton in nanostructures based on $\text{MoS}_2$

To cite this article: O O Smirnova *et al* 2020 *J. Phys.: Conf. Ser.* **1482** 012038

View the [article online](#) for updates and enhancements.

### You may also like

- [Pronounced enhancement of exciton Rabi oscillation for a two-photon transition based on quantum dot coupling control](#)  
Jian Luo, Wei Lai, Di Lu et al.
- [Temporal coherence of spatially indirect excitons across Bose–Einstein condensation: the role of free carriers](#)  
Romain Anankine, Suzanne Dang, Mussie Beian et al.
- [Electrically induced direct to indirect exciton transition in CdTe/CdMnTe concentric double quantum ring rooted in  \$\text{SiO}\_2\$  matrix](#)  
I Janet Sherly and P Nithiananthi



**ECS**  
The  
Electrochemical  
Society  
Advancing solid state &  
electrochemical science & technology

**DISCOVER**  
how sustainability  
intersects with  
electrochemistry & solid  
state science research

# Temperature activation of indirect exciton in nanostructures based on MoS<sub>2</sub>

O O Smirnova<sup>1,2</sup>, I A Elisyev<sup>2</sup>, A V Rodina<sup>2</sup> and T V Shubina<sup>2</sup>

<sup>1</sup> ITMO University, 49 Kronverkskiy pr., St. Petersburg 197101, Russia

<sup>2</sup> Ioffe Institute, 26 Politekhnicheskaya, St. Petersburg 194021, Russia

E-mail: [smirnova.olga248@gmail.com](mailto:smirnova.olga248@gmail.com)

**Abstract.** Micro-photoluminescence studies of MoS<sub>2</sub> nanotubes have shown that both direct and indirect excitonic transitions contribute to the emission spectra despite the fact that dozens of monolayers are inside their walls and, therefore, only indirect exciton emission would be expected. In addition, the intensity of the indirect exciton band increases with temperature in contrast to the direct exciton band, the intensity of which decreases. The same effects are observed for MoS<sub>2</sub> flakes. To describe these phenomena, we propose a theoretical model that considers the balance between exciton transitions taking into account the spin-forbidden exciton states.

## 1. Introduction

After a promising breakthrough in physics of the first two-dimensional (2D) crystal – graphene, a lot of effort was put into the study of monolayers of other materials. This led to the invention of 2D structures based on a large family of transition metal dichalcogenides (TMD). The most studied representative of this group is MoS<sub>2</sub>. It was shown both theoretically and experimentally that this semiconductor has an indirect band structure for bulk with a band gap of  $\sim 1.3$  eV [1]. In the limit of a monolayer, the band structure is modified and becomes direct with a band gap of  $\sim 1.9$  eV [2].

As for MoS<sub>2</sub> nanotubes synthesized in 1996 [3], it was predicted that they will be semiconducting independently on the folding type and that the multi-walled ones will have the similar properties as bulk, while the single-walled will resemble the monolayer [4]. Their structural and electrophysical properties have been actively studied in terms of their application in such fields as microfluidics, tribology and opto- and nanoelectronics [5]. However, nanotubes were never considered for the purposes of nanophotonics because their luminescent properties were generally unknown. It should be noted that the nanotubes are usually multi-walled and one can expect rather weak radiation associated with indirect exciton transitions, which are forbidden by momentum. Unexpectedly, the first micro-photoluminescence experiments with individual MoS<sub>2</sub> nanotubes [6] showed that the indirect exciton emission is completely absent at low temperatures. This emission appears at 80-100 K and increases in intensity towards room temperature, while the intensity of direct exciton radiation decreases with temperature, as usual. It is noteworthy that the flakes grown in the same growing process and exfoliated from the bulk crystal exhibit similar temperature behavior.



MoS<sub>2</sub> has a complicated structure of excitonic states that includes, besides the bright excitons, both spin and momentum forbidden (dark) ones. The mutual position of the bright and dark exciton states determines the temperature behavior of the emission yield [7]. In this paper, we propose a theoretical model which can explain the observed phenomena by the peculiarities of excitation energy transfer in the system with two types of transitions, direct and indirect in momentum space, separated in energy by  $\sim 600$  meV. By analyzing the experimental data obtained in a wide temperature range, we show that spin forbidden exciton states and interaction with phonons can play an important role in the emission process in both MoS<sub>2</sub> nanotubes and flakes.

## 2. Experimental

We studied the MoS<sub>2</sub> nanotubes and flakes grown by chemical transport reaction which produces nanostructures with an extremely low density of structural defects [8]. In addition, the flakes exfoliated from a high-quality bulk crystal (HQ Graphene production) were investigated. These studies were performed using micro-photoluminescence ( $\mu$ -PL) spectroscopy with a spatial resolution  $\sim 1 - 1.5 \mu\text{m}$  using a 532-nm laser line for excitation. Other details are described in [6, 9]. The  $\mu$ -PL spectra were measured at different temperatures, from 8 K up to room temperature. There are no differences in the temperature behavior of the exfoliated and synthesized flakes.

Typical  $\mu$ -PL spectra for the flakes and nanotubes are presented in figure 1. They show that the indirect exciton band is less pronounced in the nanotubes than in the flakes. Presumably, we associate this with the chiral architecture of nanotubes with domains containing a limited number of monolayers. Another fundamental feature is that in both tubular and planar nanostructures, the emission of the indirect exciton appears in the same range of 80 – 100 K, being almost absent at lower temperatures. This feature is also observed after special treatment of the nanostructures in an aggressive environment, which can stimulate the separation of monolayers, though the temperature at which the indirect exciton emission appears and the slope of dependencies are somewhat changed. (Below such nanostructures are denoted as "treated" in contrast to the non-treated "as-grown".) We suggest that such threshold behavior can be realized either when the lowest exciton state is dark or when phonons control the energy relaxation process.

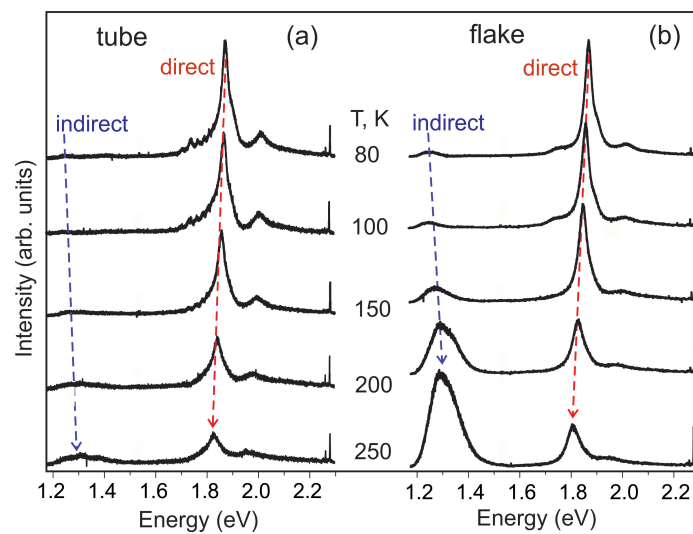


**Figure 1.** Characteristic experimental series of normalized  $\mu$ -PL spectra of a tube (a) and a flake (b), measured at different temperatures shown in the plots.

### 3. Theoretical model

The observed phenomenon is described by using a model, which includes excited levels of the direct exciton (bright ( $A$ ) is "allowed" and dark ( $F$ ) is "forbidden") and such a pair of levels corresponding to the indirect exciton. It was predicted theoretically [11] that the bright state of the direct exciton has a lower energy in MoS<sub>2</sub> than the dark one. Up to now, nothing is known about the order of levels for the indirect exciton. Here, we assume that the dark exciton state is conditionally lower in energy than the bright one. The scheme of the model with the notations of excited levels and allowed transitions is shown in figure 2.

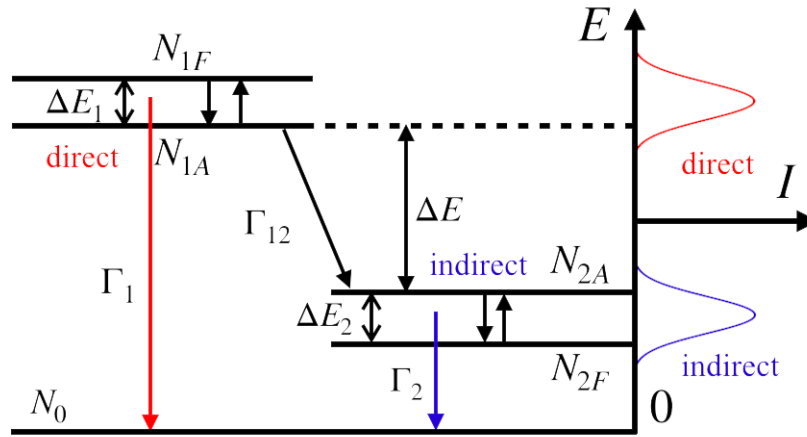


**Figure 2.** Schematic representation of the levels of the direct and indirect excitons in nanostructures based on MoS<sub>2</sub>.  $\Delta E, \Delta E_{1,2}$  are the energy distance between the corresponding levels;  $N_{i,\alpha}$  is the level population;  $i = 1, 2$ ;  $\alpha = A, F$ ;  $\Gamma_i$  is the probability of the corresponding transition. The schematic representation of the photoluminescence is shown on the right.

To begin with, we consider each subsystem as a whole. This allows us to investigate the case of a three-level system that consists of two excited states and a ground state. The system may be characterized by a parameter varying from -1 to 1:

$$P = \frac{I_1 - I_2}{I_1 + I_2}, \quad (1)$$

where  $I_{1,2}$  is the intensity of direct and indirect exciton photoluminescence, respectively, under constant wave pumping.  $I_{1,2} = \Gamma_{1,2}^{\text{rad}} N_{1,2}$ , where  $\Gamma_{1,2}^{\text{rad}}$  is the radiative recombination rate,  $N_{1,2}$  is the subsystem stationary population.

In order to rewrite the expression (1) in a convenient for analysis form, we invent a parameter  $\xi$ , which describes the entire temperature dependence in the considered system:

$$\xi = \frac{I_2}{I_1} = \frac{\Gamma_2^{\text{rad}} N_2}{\Gamma_1^{\text{rad}} N_1}. \quad (2)$$

In terms of this parameter, the temperature dependence of  $P$  can be written as:

$$P(T) = \frac{1 - \xi(T)}{1 + \xi(T)}. \quad (3)$$

The populations can be obtained by finding a solution to the rate equations for the case of constant wave pumping:

$$\begin{cases} \frac{\partial N_1}{\partial t} = -(\Gamma_1 + \Gamma_{12})N_1 + \Gamma_{21}N_2 + G_1 \\ \frac{\partial N_2}{\partial t} = \Gamma_{12}N_1 - (\Gamma_2 + \Gamma_{21})N_2 + G_2 \end{cases}, \quad (4)$$

where  $\Gamma_{12}, \Gamma_{21}$  are the relaxation rates between subsystems,  $\Gamma_{1,2}$  are the recombination rates of the direct and indirect excitons (figure 2). In general, the recombination rates  $\Gamma_i$  include both radiative ( $\Gamma_i^{\text{rad}}$ ) and non-radiative ( $\Gamma_i^{\text{nr}}$ ) quiting.  $G_1, G_2$  are the populations excited by pumping per time unit. According to the experimental conditions, we assume that pumping only populates the levels of the direct exciton  $N_{1A,1F}$  ( $G_2 = 0$ ). Due to the large energy distance between the direct and indirect excitons, we also suppose relaxation between subsystems goes only down in energy ( $\Gamma_{21} = 0$ ). By solving the rate equations in the described approximations, we obtain the stationary state solution:

$$\frac{N_2}{N_1} = \frac{\Gamma_{12}}{\Gamma_2}. \quad (5)$$

Therefore, the parameter  $\xi$  can be rewritten as follows:

$$\xi = \frac{\Gamma_2^{\text{rad}}}{\Gamma_2} \frac{\Gamma_{12}}{\Gamma_1^{\text{rad}}}. \quad (6)$$

The first factor in  $\xi$  is responsible for the efficiency of the indirect exciton transition, and the second shows the ratio between the relaxation rate and the radiative rate of the direct exciton transition.

Now we take into account that both exciton systems include two sublevels - dark ( $F$ ) and bright ( $A$ ) states. The effect of this is presented in the influence of the relative population of the levels on the radiative transition probability.

$$\Gamma_1^{\text{rad}} = \frac{\Gamma_{1A}N_{1A}}{N_{1A} + N_{1F}}, \quad (7)$$

where  $N_{1A,F}$  is the level population,  $\Gamma_{1A}$  is the rate of the direct bright exciton. The same is true for  $\Gamma_2^{\text{rad}}$  with the change  $1 \rightarrow 2$ .

We assume that the relaxation between sublevels is very fast. That allows us to consider the subensembles in their equilibrium states, when the population ratio is given by the equilibrium value  $N_{1A}/N_{1F} = \exp(\Delta E_1/(kT))$ , where  $\Delta E_1 > 0$  is the energy splitting between dark and bright excitonic states in subensemble of the direct exciton,  $k$  is the Boltzmann constant. For the indirect exciton  $N_{2A}/N_{2F} = \exp(-\Delta E_2/(kT))$ , where  $\Delta E_2 > 0$ . Under these assumptions, the ratio  $\Gamma_2^{\text{rad}}/\Gamma_2$  takes on the form:

$$\frac{\Gamma_2^{\text{rad}}}{\Gamma_2} = \frac{\Gamma_2^{\text{rad}}}{\Gamma_2^{\text{nr}} + \Gamma_2^{\text{rad}}} = \frac{\Gamma_{2A}/\Gamma_2^{\text{nr}}}{\Gamma_{2A}/\Gamma_2^{\text{nr}} + 1 + e^{\frac{\Delta E_2}{kT}}}. \quad (8)$$

The temperature dependence we use for the fitting is:

$$\xi = A \frac{e^{-\frac{\Delta E_1}{kT}} + 1}{e^{\frac{\Delta E_2}{kT}} + 1 + d}, \quad (9)$$

where  $d = \Gamma_{2A}/\Gamma_2^{\text{nr}}$ ,  $A = \Gamma_{12}/\Gamma_{1A}d$ . In the first approximation, we assume that  $A$  is temperature independent.

#### 4. Results and discussion

The fitting of the experimental dependencies measured in the as-grown and treated nanostructures is presented in figures 3 and 4. The parameters gained from the fitting showed some interesting values. In the initial not-treated nanostructures,  $\Delta E_1$  has a value of about 50 meV, which is close to the energy of optical phonons. That can probably tell us about the involvement of optical phonons in the excitation transfer from the direct exciton levels in a multilayer close-packed system. In this case, the optically dark states related to the large wavevectors outside the light cone are dominating [10] and their activation needs phonons. In nanostructures that underwent the treatment which increases their interplanar spacing, the parameter  $\Delta E_1$ , which was initially determined for the splitting between the bright and dark states of the direct exciton, gives 2 – 3 meV. This value is well consistent with the literature data for dark-bright exciton splitting in isolated monolayers of MoS<sub>2</sub> [11]. In this condition, the radiative recombination rate of the direct exciton possessing large oscillator strength is high, and the direct transition dominates over the indirect one.

As for  $\Delta E_2$ , its variation in as-grown and treated nanostructures is within the limits of experimental accuracy. However, it decreases almost twice from  $\sim 100$  meV in flakes to  $\sim 50$

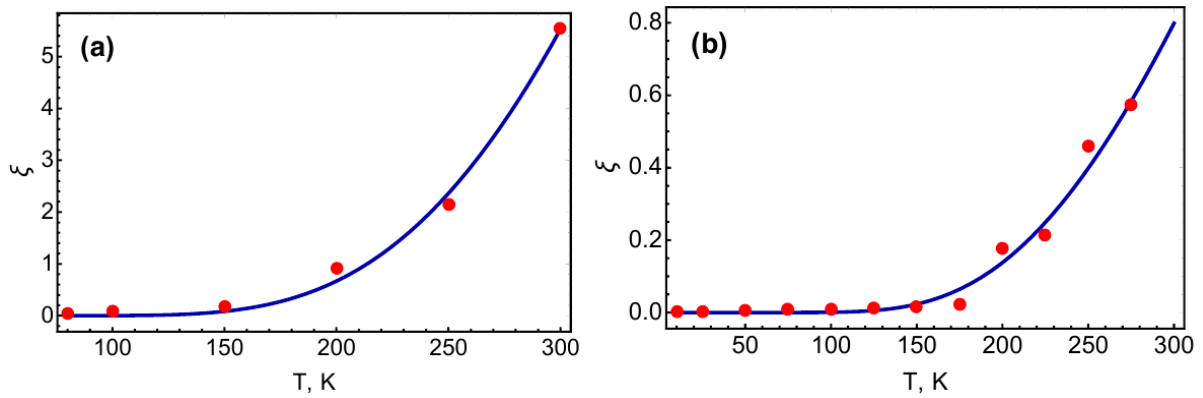


**Figure 3.** The fitting of experimental dependencies using equation (9) for a flake (a) as-grown, (b) treated with the following parameters: (a)  $\Delta E_1 = 51$  meV,  $\Delta E_2 = 106$  meV,  $A = 298$ ,  $d = 0.01$ , (b)  $\Delta E_1 = 3.5$  meV,  $\Delta E_2 = 91$  meV,  $A = 15$ ,  $d = 0.4$

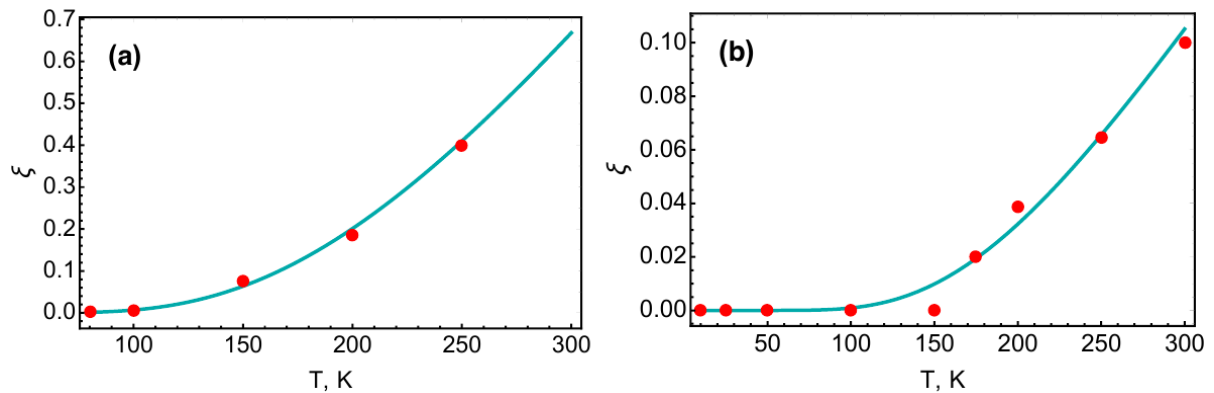


**Figure 4.** The fitting of experimental dependencies using equation (9) for a tube (a) as-grown, (b) treated with the following parameters: (a)  $\Delta E_1 = 40$  meV,  $\Delta E_2 = 57$  meV,  $A = 5$ ,  $d = 0.01$ , (b)  $\Delta E_1 = 1.9$  meV,  $\Delta E_2 = 60.5$  meV,  $A = 0.57$ ,  $d = 0.08$

meV in tubes. We highlight that these values are multiples of the optical phonon energy as well. A decrease in their number (one phonon instead of two) may evidence a simplification of the phonon-assisted mechanism. On the other hand, the  $\sim 100$  meV value is close to the energy separation between the indirect transitions from  $K$  point and an "intermediate" point to  $\Gamma$ . Thus, it may also evidence a change in the way of energy relaxation between the tubes and flakes, which needs further investigation.

The parameter  $A$  significantly drops after the treatment both in flakes and tubes; it decreases also in the tubes with respect to the flakes. In part, that can be because the rate of the bright exciton,  $\Gamma_{1A}$ , increases significantly as expected for the monolayers with respect to bulk. (This is one more argument in favor of monolayer separation.) As for the parameter  $d$ , due to the large splitting  $\Delta E_2$ , it can take values in a certain range ( $0.01 < d < 20$ ) that slightly changes  $A$ . We assume that the experiment with variable wavelength of excitation, above and below the direct exciton energy, will be very useful to make the final conclusion on the mechanism of the energy transfer in MoS<sub>2</sub> nanostructures.

In conclusion, the performed modeling of the experimental data allows us to analyze the excitation transfer mechanism in MoS<sub>2</sub> nanostructures. The differences in the optical properties of as-grown and treated tubes and flakes are explained in terms of radiation and energy transfer rates.

## Acknowledgements

The work was supported by the Russian Science Foundation (project # 19-12-00273). The authors thank V. Yu. Davydov and A. A. Toropov for the fruitful discussions.

## References

- [1] Wilson J A and Yoffe A D 1969 *Adv. Phys.* **18** 193
- [2] Mak K F, Lee C, Hone J, Shan J and Heinz T F 2010 *Phys. Rev. Lett.* **105** 136805
- [3] Remškar M, Skraba Z, Cléton F, Sanjinés R, and Lévy F 1996 *Appl. Phys. Lett.* **69**, 351
- [4] Seifert G, Terrones H, Terrones M, Jungnickel G and Frauenheim T 2000 *Phys. Rev. Lett.* **85** 146
- [5] Zhang C, Wang S, Yang L, Liu Y, Xu T, Ning Z, Zak A, Zhang Z, Tenne R and Chen Q 2012 *Appl. Phys. Lett.* **100** 243101
- Fathipour S et al. 2015 *App. Phys. Lett.* **106** 022114
- [6] Shubina T V, Remškar M, Davydov V Yu, Belyaev K G, Toropov A A and Gil B 2019 *Annalen der Physik* **531** 1800415
- [7] Malic E, Selig M, Feierabend M, Brem S, Christiansen D, Wendler F, Knorr A and Berghuser G 2018 *Phys. Rev. Materials* **2** 014002
- [8] Remškar M 2004 *Adv. Mater.* **16** 1497
- [9] Kazanov D R et al. 2018 *Appl. Phys. Lett.* **113** 101106
- [10] Andreani L C, Tassone F and Bassani F 1991 *Solid State Commun.* **77**, 641
- [11] Durnev M V and Glazov M M 2018 *Phys. Usp.* **61** 825